(Received 24 September 2025, Accepted 13 November 2025, Scheduled 6 January 2026)

A Simple Structure of High-Gain Dual-Beam Fabry-Perot Antenna Design

Chang-Yi Yi and Yan-Fei Li*

School of Information and Communication Engineering, Communication University of China, Beijing, China

ABSTRACT: Beam steering antennas are advanced technologies used for directing radio waves in a specific direction without physically moving the antenna. In this paper, a simple two-steering-beam antenna is designed based on a Fabry-Perot structure. The amplitude and phase control theory is introduced to design the electric field phase and electric field strength in the near field to obtain the far-field radiation pattern required for the Fabry-Perot antenna (FPA). The FPA working at 10 GHz with the aperture of $5\lambda_0 \times 5\lambda_0$ steers to $\pm 30^\circ$ with the maximum gain of 18 dB for each beam realized by a proper design of the superstrate, which is a key to realizing a beam-steering antenna with a simple structure.

1. INTRODUCTION

At present, beam control is mainly realized by using reflection metasurfaces, transmission metasurfaces, and antenna arrays. However, in order to achieve the effect of beam control precisely, plane waves or spherical waves are required as the excitation of the metasurface, while the antenna array needs to be excited by a feed network composed of power dividers, couplers, feed ports, and many units to achieve high gain. Therefore, the Fabry-Perot antenna, which combines the characteristics of high gain and simple feeding, has attracted more and more attention. Extensive research has been conducted on the high gain of FPAs [1]. According to the traditional array antenna theory, it is difficult to achieve beam steering by changing the intensity and phase of a single-feed FP resonator. Therefore, it is of great significance to explore alternative ways to achieve beam control of FPA. Hao et al. achieved beamforming by biasing the feed within the resonator antenna [2]. Ourir et al. achieved a 20° beam scanning range by changing the spacing between the metal strips to control the reflection phase of the superstrate [3]. Sun et al. presented a high-gain, low-profile subwavelength substrate-integrated Fabry-Pérot cavity antenna using artificial magnetic conductor sheets, which reduces antenna thickness with a fully dielectric substrate and improves radiation patterns [4]. Feresids et al. explored the use of single-layer artificial magnetic conductor (AMC) arrays in high-gain, low-profile planar antennas, combining ray theory and full-wave analysis to reduce antenna profile and improve performance [5]. Wang et al. configured a single reflection mode (R-mode) Fabry-Perot cavity (FPC) and two external feed antennas operating in the same frequency band, and achieved a beam scan angle of 30° per beam by independently changing the irradiation angle of the two feeds to the R-type FPC. However, the feeding method of this antenna is more complicated, and the essence is that one feed point corresponds to a beam [6]. Singh and Park designed a dual-beam high-gain antenna by placing a lens composed of two identical stacked metasurface layers on the top of the radiator, resulting in a broad side gain of 13.5 dBi at 28 GHz [7]. Yu and Zheng designed a compact switched dual-beam array antenna operating at 5.8 GHz. The antenna is fed by an innovative dual-beam beamforming network to achieve high gain. By exciting its separate input ports, the array generates two distinct beams whose main directions are steered to $\pm 26^\circ$. The measured gain of each beam is 9.7 dBi [8]. Bashir et al. proposed a high-gain dual-beam digitally coded Huygens Metasurface Lens (HML) antenna for mmWave applications. The antenna combines a digitally encoded Huygens metasurface with the assembly of a metasurface lens and patch antenna to achieve a dual-beam radiation pattern. In the azimuth plane ± 37 GHz, there is a double beam radiation along 10°, and a peak gain of 16.7 dBi is obtained [9]. Zhang et al. controlled the main lobe direction through phase compensation technology and combined the Schelkunoff polynomial with the actual radiation amplitude of the feed to control the reflection amplitude of the metasurface, achieving a metasurface design with independently adjustable amplitude and phase [10]. Dave and Franklin studied a metasurface for 13.6 GHz, which is fed by a planar source antenna. By changing the near-field phase, the beam direction and gain were affected, achieving dual beams with deflections of 34° each. The gain of each dual beam is approximately 11 dBi [11]. In total, all of these studies necessitate altering the feed location or feed method, using complex cell units, or even incorporating intricate polymetallic to precisely control the radiation phase.

Therefore, current research for achieving advanced beam control and multi-functional integration in FPAs consistently demands alterations to the feed location or method [2, 6, 8, 10, 14], the use of complex unit cells [3, 16–18], or the implementation of intricate hybrid systems and array architectures [12, 13, 15]. While these methods achieve excellent performance, they significantly increase the com-

* Corresponding author: Yanfei Li (liyanfei@cuc.edu.cn).

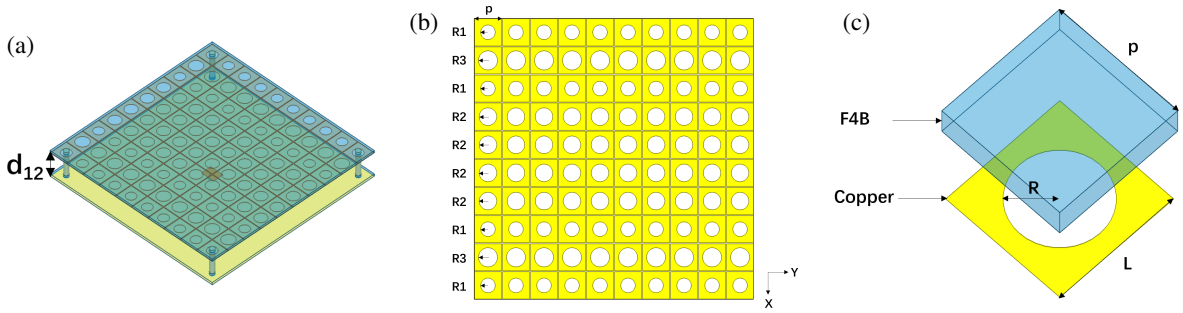

FIGURE 1. Dual-beam Fabry-Perot resonator antenna: (a) Overall picture; (b) Upper copper patch; (c) Unit cell.

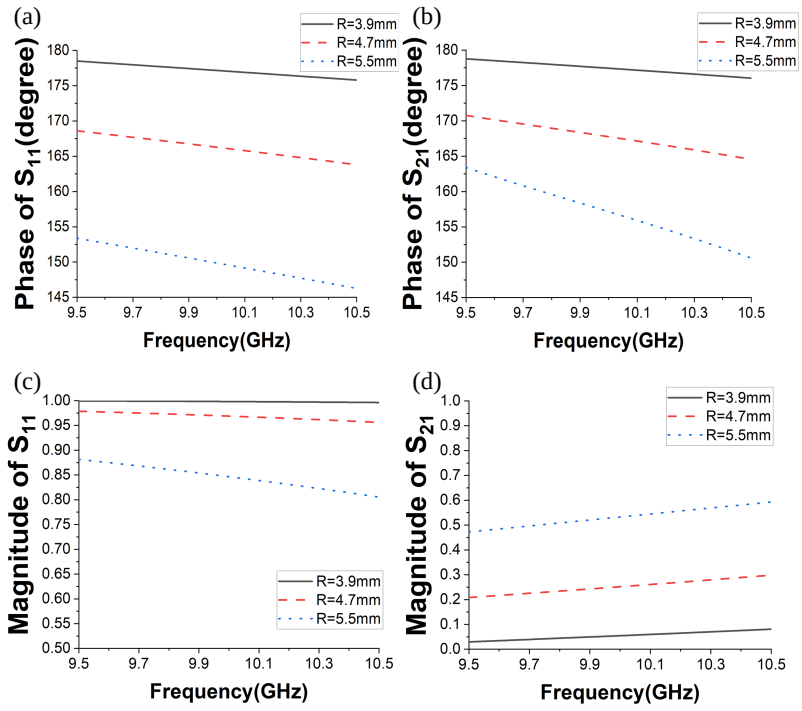

FIGURE 2. Properties of three holed patch units: (a) Phase and (b) Magnitude.

plexity and manufacturing cost of the antenna. Therefore, exploring a novel, low-complexity design that can achieve high-gain dual-beam functionality while maintaining a simple single-feed structure is of significant engineering and academic importance.

In this paper, a simple and easy-to-implement antenna structure based on square patch elements with drilled holes is proposed to achieve amplitude and phase control. By carefully adjusting the size of each hole, the near-field electric-field magnitude and phase are tailored to achieve aperture-size modulation, enabling effective far-field beam shaping. Using this approach, dual beams can be steered to $\pm 30°$, each reaching a gain of approximately 18 dBi, without increasing structural or feeding complexity.

2. DUAL-BEAM FABRY-PEROT ANTENNA DESIGN

2.1. Antenna Configuration

An FPA working at 10 GHz has been designed here. The design and simulations were carried out using High Frequency Structure Simulator (HFSS). The antenna consists of a Partial Reflective Surface (PRS)-Superstrate, a ground plane, and a patch antenna, which would realize dual-beam steering at $\pm 30°$, as shown in Fig. 1(a). The PRS structure comprises a 10×10 array of unit cells, with overall dimensions of 150 mm $\times$ 150 mm ($5\lambda_0 \times 5\lambda_0$), where the periodic size p of unit cell is 15 mm. Each unit cell consists of a copper patch with a central hole, printed on a substrate, as shown in Fig. 1(b) and Fig. 1(c).

The PRS is composed of an uneven-aperture holed PRS patch, which was designed to meet the near-field distribution requirements, enabling beam steering to $\pm 30°$ in the far field. The detailed distribution of the holed patch array in the PRS is shown in Fig. 1(b) with radius $R_1 = 3.9$ mm, $R_2 = 4.7$ mm, and $R_3 = 5.5$ mm. Each patch element has a side length of $L = 14.5$ mm. The lower layer of the PRS-superstrate is the holed patch, which is oriented toward the patch antenna. The separation between the patch antenna and the PRS is denoted as d_{12} and as mentioned above, set to 14.6 mm.

The X-polarized patch antenna is designed with a dimension of 11.29 mm $\times$ 8.58 mm. Both the substrate of patch antenna

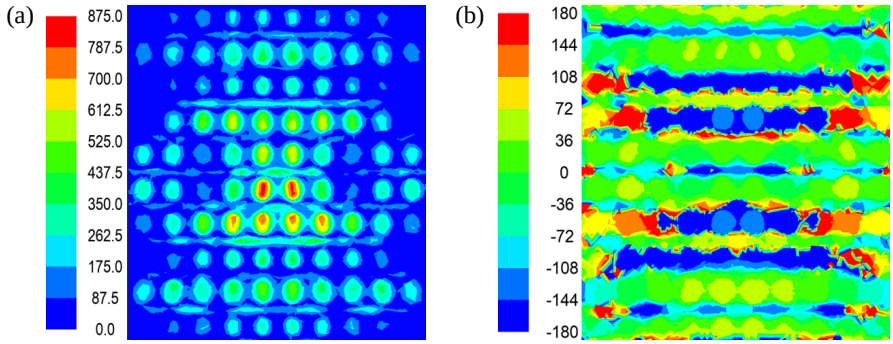

FIGURE 3. E-field distribution on the plane of the holed patch array at 10 GHz: (a) Magnitude distribution; (b) Phase distribution.

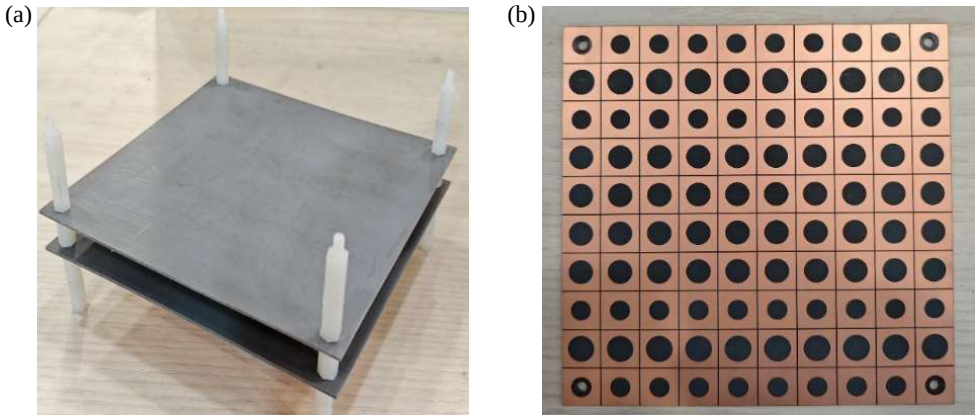

FIGURE 4. Fabricated antenna of the Fabry-Perot resonator: (a) Assembled structure; (b) Holed patch array PRS superstrate.

and the superstrate dielectric of the holed PRS use F4B dielectric, which has a relative permittivity of 2.2 and a thickness of 1.5 mm.

2.2. Realization of the 30-Degree Dual Beams

The designing process, achieved by adjusting the aperture sizes of the holes in the superstrate, effectively modulates the amplitude and phase of the outgoing field, resulting in the steering of the beam to $\pm 30°$. The quantitative analysis of the electric field phase and amplitude corresponding to various aperture sizes is as follows. We can see that the magnitude and phase measured according to the s-parameters exhibit linear variations within specific frequency bands, which allows us to precisely control the magnitude e phase. The characteristics of the three unit cells are illustrated in Fig. 2. We can see that at a frequency of 10 GHz, the transmission and reflection phases are apart, and the transmission coefficient and reflection coefficient also change when the radii are R_1 (3.9 mm), R_2 (4.7 mm), and R_3 (5.5 mm). Based on this, we designed the PRS shown in Fig. 1(b) as the superstrate for the FP antenna. The hole size varies along the x-direction while remaining constant along the y-direction. Specifically, at 10 GHz, the S_{11} phases corresponding to R_1 (3.9 mm), R_2 (4.7 mm), and R_3 (5.5 mm) are 176°, 166°, and 151°, with normalized S_{11} amplitudes of 0.99, 0.97, and 0.85. The S_{21} phases are 177°, 167°, and 157°, with normalized S_{21} amplitudes of 0.09, 0.24, and 0.53, respectively.

FIGURE 5. Test environment of the Fabry-Perot resonator antenna.

Figure 3 shows both the amplitude and phase distribution of the x-polarized E-field components of the designed FPA on the holed patch array. This variation in hole size causes the phase and amplitude of the electromagnetic waves emerging from the FP cavity to differ from those of a uniform superstrate structure. Consequently, two beams are generated along the x-direction. By adjusting the differences in hole sizes, beam steering at different angles can be achieved.

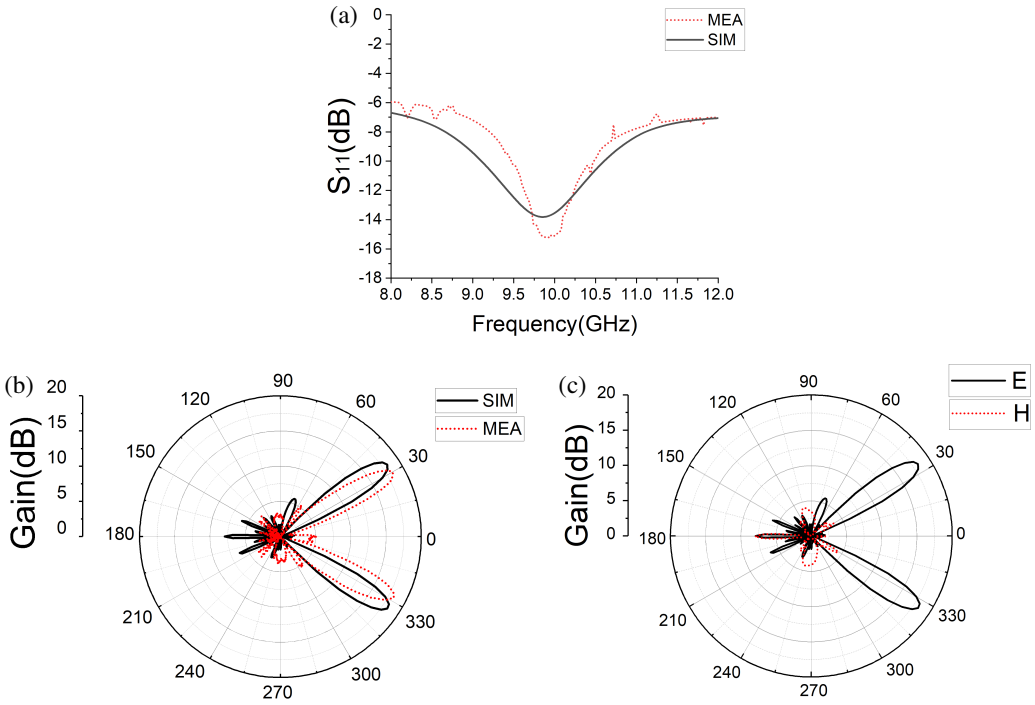

FIGURE 6. Simulation and measurement results of the designed FPA: (a) S_{11} result of the Fabry-Perot resonator antenna; (b) Antenna E plane radiation pattern at 10 GHz; (c) Antenna simulation result of E plane and H plane radiation pattern at 10 GHz.

TABLE 1. Comparison between the proposed dual-beam antenna and recently reported designs.

Reference	Frequency (GHz)	Gain (dBi)	Beam Steering	Structure Type	Feeding Method	Key Feature
[7]	28	13.5	$\pm10^\circ$	Double-layer metasurface lens	Dual-feed	Moderate gain, narrow beam deflection
[8]	5.8	9.7	$\pm26^\circ$	Compact array with beamforming network	Multi-port feed	Requires complex beamforming network
[9]	37	16.7	$\pm10^\circ$	Digitally coded Huygens metasurface	Single feed	High frequency, limited beam range
This work	10	18.0	$\pm30^\circ$	Single-layer holed PRS Fabry-Perot cavity	Single-feed	Wide-angle dual beams with high gain and simple structure

3. FABRICATION AND MEASUREMENTS

The fabricated antenna is shown in Fig. 4, where Fig. 4(a) presents the overall assembled structure, and Fig. 4(b) displays the holed patch array PRS superstrate. Since the holed array faces the excitation source (patch antenna), it is not visible in Fig. 4(a). The antenna was measured in a microwave anechoic chamber using an ENA Series network analyzer (Agilent E5071C (300 kHz–20 GHz)), as shown in Fig. 5.

The simulated and measured S_{11} of the FP antenna are shown in Fig. 6(a), while the simulated and measured E-plane radiation patterns at 10 GHz are presented in Fig. 6(b), and total radiation patterns at 10 GHz are presented in Fig. 6(c). It is evident that dual beams at $\pm30^\circ$ are successfully realized in the E-plane, with a peak gain of 18 dBi. Both the sidelobe and backlobe levels are suppressed to less than 5 dBi. The measurement results are in good agreement with the simulation ones.

To further evaluate the performance superiority of the proposed design, a comparison between the presented dual-beam antenna and recently reported works is summarized in Table 1. As can be seen, the proposed Fabry-Perot antenna achieves a dual-beam steering of $\pm30^\circ$ with a peak gain of 18 dBi at 10 GHz, which represents a notable enhancement in both beam deflection and radiation performance compared with previous designs. Specifically, the antennas reported in [7–9] exhibit either limited beam scanning angles ($\pm10^\circ$–$\pm26^\circ$) or moderate gains (below 17 dBi), often relying on multi-layer metasurface lenses or complex multi-feed beamforming networks.

4. CONCLUSION

A high-gain dual-beam Fabry-Perot antenna based on a single-layer holed partially reflective surface (PRS) has been proposed and demonstrated. By precisely controlling the near-field amplitude and phase through hole-size modulation, the antenna achieves effective far-field beam shaping without increasing structural or feeding complexity. The fabricated prototype operating at 10 GHz with an aperture of $5\lambda_0 \times 5\lambda_0$ exhibits dual-beam steering at $\pm 30^\circ$ and a measured peak gain of 18 dBi. These results verify that the proposed amplitude-phase control strategy enables compact, high-efficiency beam-steering antennas with excellent radiation performance.

REFERENCES

[1] Lu, Y.-F. and Y.-C. Lin, "A hybrid approach for finite-size Fabry-Pérot antenna design with fast and accurate estimation on directivity and aperture efficiency," *IEEE Transactions on Antennas and Propagation*, Vol. 61, No. 11, 5395–5401, Nov. 2013.

[2] Hao, Y., A. H. Alomainy, and C. G. Parini, "Antenna-beam shaping from offset defects in UC-EBG cavities," *Microwave and Optical Technology Letters*, Vol. 43, No. 2, 108–112, 2004.

[3] Ourir, A., S. N. Burokur, and A. de Lustrac, "Phase-varying metamaterial for compact steerable directive antennas," *Electronics Letters*, Vol. 43, No. 9, 493–494, Apr. 2007.

[4] Sun, Y., Z. N. Chen, Y. Zhang, H. Chen, and T. S. P. See, "Sub-wavelength substrate-integrated Fabry-Pérot cavity antennas using artificial magnetic conductor," *IEEE Transactions on Antennas and Propagation*, Vol. 60, No. 1, 30–35, Jan. 2012.

[5] Feresidis, A. P., G. Goussetis, S. Wang, and J. C. Vardaxoglou, "Artificial magnetic conductor surfaces and their application to low-profile high-gain planar antennas," *IEEE Transactions on Antennas and Propagation*, Vol. 53, No. 1, 209–215, Jan. 2005.

[6] Wang, Q., C. Pang, and J. Qi, "A novel dual-beam high gain beam scanning Fabry-Pérot cavity antenna based on bidirectional asymmetric transmission metasurface," in *2024 IEEE International Symposium on Antennas and Propagation and INC/USNC-URSI Radio Science Meeting (AP-S/INC-USNC-URSI)*, 1157–1158, Firenze, Italy, 2024.

[7] Singh, A. K. and S.-O. Park, "Dual beam high gain antenna for 5th generation communication system using metasurface lens," in *2019 8th Asia-Pacific Conference on Antennas and Propagation (APCAP)*, 456–457, Incheon, Korea (South), 2019.

[8] Yu, C. and S. Y. Zheng, "A compact switched dual-beam antenna array with high gain," in *2021 IEEE Conference on Antenna Measurements & Applications (CAMA)*, 31–34, Antibes Juan-les-Pins, France, 2021.

[9] Bashir, G., A. K. Singh, and N. Bhartiya, "Dual beam high gain digitally coded huygens metasurface lens antenna for millimeter wave applications," in *2024 IEEE International Symposium on Antennas and Propagation and INC/USNC-URSI Radio Science Meeting (AP-S/INC-USNC-URSI)*, 1039–1040, Firenze, Italy, 2024.

[10] Zhang, P., W. Zhang, X. Chen, G. Han, J. Su, and R. Yang, "Low-sidelobe dual-beam antenna based on metasurface with independently regulated amplitude/phase," *IEEE Antennas and Wireless Propagation Letters*, Vol. 22, No. 10, 2382–2386, Oct. 2023.

[11] Dave, A. and R. Franklin, "Single feed dual beam antenna using metamaterial surfaces for near-field phase manipulation," in *2021 IEEE International Symposium on Antennas and Propagation and USNC-URSI Radio Science Meeting (APS/URSI)*, 621–622, Singapore, 2021.

[12] Khang, G. G., S. J. Kim, and D. Kim, "High-gain Fabry-Pérot cavity antenna with an artificial magnetic conductor side wall," *IEEE Antennas and Wireless Propagation Letters*, Vol. 22, No. 9, 2245–2249, Sep. 2023.

[13] Wang, Q., Y. Wang, A. Sihvola, and J. Qi, "Aperture-shared dual-band high-gain beam-scanning antenna hybridizing reflection-mode Fabry-Pérot cavity and wide-angle reflectarray," *IEEE Antennas and Wireless Propagation Letters*, Vol. 23, No. 7, 2021–2025, Jul. 2024.

[14] Shahzadi, I., D. Comite, M. V. Kuznetcov, and S. K. Podilchak, "Compact dual-polarized Fabry-Pérot leaky-wave antenna for full-duplex broadband applications," *IEEE Antennas and Wireless Propagation Letters*, Vol. 23, No. 9, 2693–2697, Sep. 2024.

[15] Gu, L., W. Yang, Q. Xue, and W. Che, "A ±45° dual-polarized dual-beam series-fed metasurface antenna array with stable beam angle," *IEEE Transactions on Antennas and Propagation*, Vol. 69, No. 12, 8366–8375, Dec. 2021.

[16] Fang, S., L. Zhang, Y. Guan, Z. Weng, and X. Wen, "A wideband Fabry-Pérot cavity antenna with single-layer partially reflective surface," *IEEE Antennas and Wireless Propagation Letters*, Vol. 22, No. 2, 412–416, Feb. 2023.

[17] Chatterjee, A., K. Dutta, S. Chakrabarti, and R. Mittra, "Advanced design of high-gain Fabry-Pérot cavity antenna offering wide common impedance and gain bandwidth," *IEEE Antennas and Wireless Propagation Letters*, Vol. 22, No. 5, 1214–1218, May 2023.

[18] Yin, J., Q. Lou, H. Wang, Z. N. Chen, and W. Hong, "Broadband dual-polarized single-layer reflectarray antenna with independently controllable 1-bit dual beams," *IEEE Transactions on Antennas and Propagation*, Vol. 69, No. 6, 3294–3302, Jun. 2021.